JOURNAL OF GEOPHYSICAL RESEARCH, VOL. 87, NO. A7, PAGES 5169–5183, JULY 1, 1982

Ion Temperature Variations in the Daytime High-Latitude *F* Region

R. W. SCHUNK AND J. J. SOJKA

Center for Atmospheric and Space Sciences, Utah State University, Logan, Utah, 84322

We improved our high-latitude ionospheric model by including thermal conduction and diffusion-thermal heat flow terms in the ion energy equation so that we could study the ion temperature variations in the daytime high-latitude *F* layer in a region poleward of the auroral oval for steady state conditions at local noon. From our study we found that (1) The variation of T_i with solar cycle, season, and geomagnetic activity closely follows the T_n variation. The general trend is for higher temperatures in summer than in winter, at solar maximum than at solar minimum, and for active magnetic conditions than for quiet conditions. However, T_i changes by less than 600°K over the range of conditions considered; (2) Meridional electric fields act to heat the ion gas, and electric fields greater than 40 mV m^{-1} can cause a larger T_i change than that due to solar cycle, seasonal, and geomagnetic activity variations; (3) In the presence of meridional electric fields, there is an upward flow of heat from the lower ionosphere that acts to raise T_i at high altitudes; (4) Zonal electric fields affect T_i indirectly through changes in the electron density, but the effect can be larger than that associated with solar cycle, seasonal, and geomagnetic activity variations; (5) Diffusion-thermal heat flow affects T_i by at most 500°K; (6) Typically, T_e has a much smaller effect on T_i at high latitudes than at middle and low latitudes.

1. INTRODUCTION

Recently, we have developed a comprehensive model of the convecting high-latitude ionosphere in order to determine the extent to which various chemical and transport processes affect the ion composition and electron density at *F* region altitudes [cf. *Schunk and Raitt,* 1980; *Sojka et al.,* 1981*a,b*]. Our numerical model produces time dependent, three-dimensional ion density distributions for the ions NO^+, O_2^+, N_2^+, O^+, N^+, and He^+. The model takes account of diffusion, thermospheric winds, electrodynamic drifts, polar wind escape, energy dependent chemical reactions, magnetic storm induced neutral composition changes, and ion production due to solar EUV radiation and energetic particle precipitation.

In this investigation, we have improved our high-latitude ionospheric model by including thermal conduction and diffusion-thermal heat flow terms in the ion energy equation so that we could study the ion temperature variations in the daytime high-latitude *F* region. We studied how the daytime ion temperature varies with season, solar cycle, geomagnetic activity, convection electric field strength, the vertical ionization drift velocity, and an assumed downward heat flux at high altitudes. In addition, we studied the ion energy balance in an effort to determine the relative importance of thermal conduction, diffusion-thermal heat flow, and collisional coupling to the electrons and neutrals. The calculations were performed for a location poleward of the auroral zone (geographic latitude 73°N) for steady state conditions at local noon. The electron and neutral temperature profiles were not calculated by the model, but were supplied to the model.

Although a significant effort has been devoted to studying ion temperature variations at middle and low latitudes [c.f. *Banks and Kockarts,* 1973], in comparison much less effort has been devoted to studying the *F* region ion temperature at high-latitude. The limited experimental information available at this time indicates that there is a strong correlation between enhanced ion temperatures and large DC electric fields [*Watkins and Banks,* 1974; *St.-Maurice et al.,* 1976; *Rees et al.,* 1980; *De la Beaujardiere et al.,* 1981, *Kelley and Wickwar,* 1981; *St.-Maurice and Hanson,* 1982], and this is in general agreement with that expected theoretically [*Rees and Walker,* 1968; Roble and Dickinson, 1972; *Bank et al.,* 1974; *Schunk et al.,* 1975]. Currently, however, there are no measurements of the seasonal solar cycle or geomagnetic activity variations of the *F* region ion temperature, and altitude profiles of ion temperature are available only over a limited altitude range. Consequently, at this time it is not possible to test most of our theoretical predictions of ion temperature behavior, but our results should serve as a useful guide to future studies of the high-latitude *F* region ion temperature.

2. IONOSPHERIC MODEL

The complete description of our high-latitude ionospheric model is given elsewhere [*Schunk and Raitt,* 1980; *Sojka et al.,* 1981*a,b*] and will not be repeated here. Briefly, we follow a field tube of plasma as it convects through a moving neutral atmosphere. Altitude profiles of the ion densities are obtained by solving the appropriate continuity, momentum, and energy equations including numerous high-latitude processes. By following many field tubes of plasma, we can construct a time- dependent three-dimensional model of the high-latitude ionosphere. In this regard it should be noted that similar, although less comprehensive, models of the high-latitude *F*-region have been developed by *Knudsen et al.* [1977] and *Watkins* [1978].

For this study, we have improved our high-latitude ionospheric model by including thermal conduction and diffusion-thermal heat flow terms in the ion energy equa-

Paper number 2A0481.
0148-0227/82/002A-0481$05.00

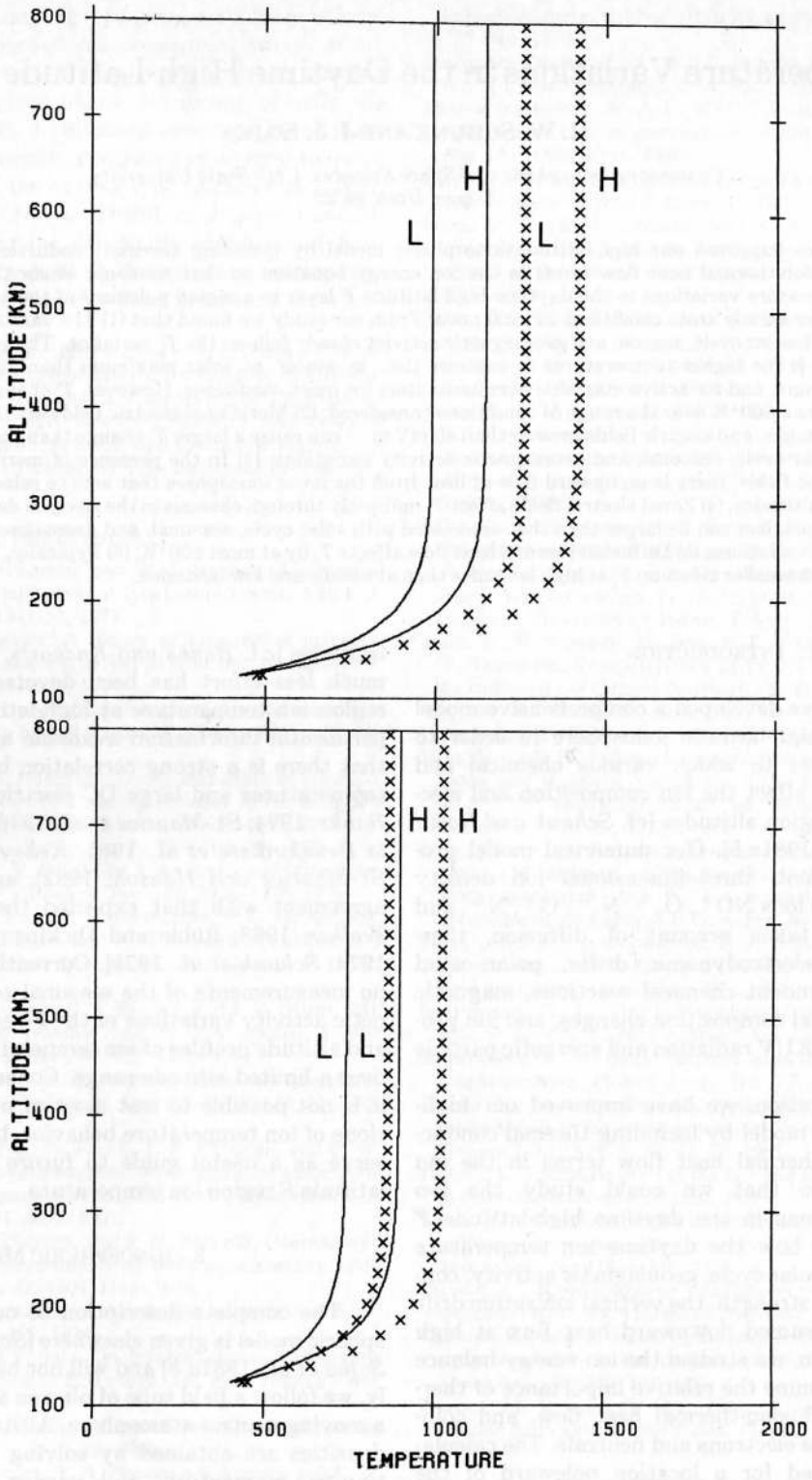

Fig. 1. Neutral temperature (°K) profiles for solar maximum (top panel) and solar minimum (bottom panel), for summer (x curves) and winter (solid curves), and for high (H) and low (L) geomagnetic activity. These temperature profiles were calculated from the MSIS model of the neutral atmosphere [*Hedin et al.*, 1977*a*, *b*].

tion so that we could study the ion temperature variations in the daytime high-latitude F region. In the paragraphs that follow, we briefly discuss the improvement to our ionospheric model.

2.1. Ion Energy Equation

With allowance for thermal conduction and diffusion-thermal heat flow, the ion energy equation takes the form [*Schunk*, 1977]

$$\frac{D_i}{Dt}\frac{(3p_i)}{2} + \nabla \cdot \mathbf{q}_i = \sum_j \frac{N_i M_i \nu_{ij}}{M_i + M_j}\left[3k(T_j - T_i)\Psi_{ij} + M_j(\mathbf{U}_i - \mathbf{U}_j)^2 \Phi_{ij}\right] \quad (1)$$

where N_i is the ion density, M_i is the mass, T_i is the

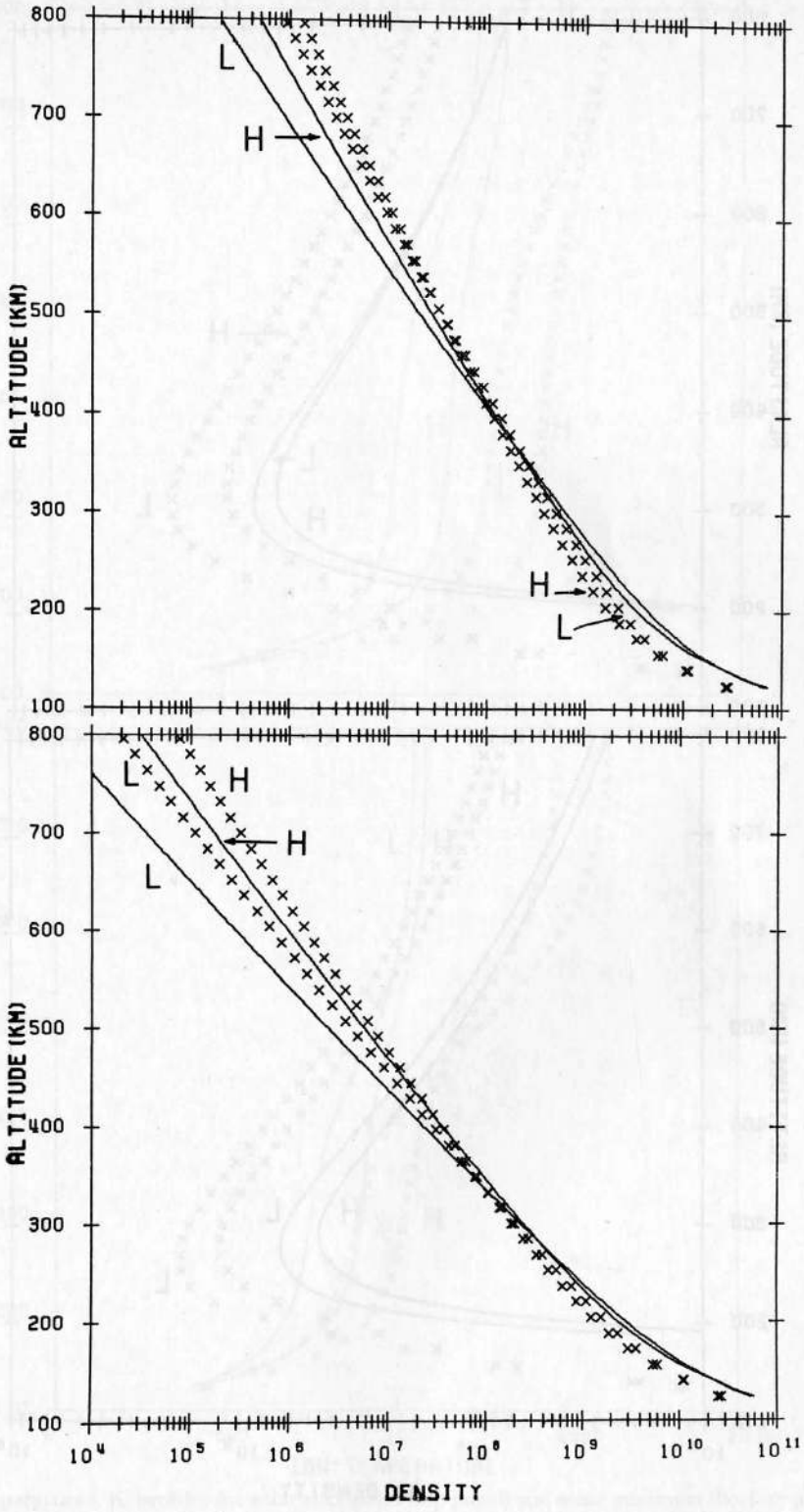

Fig. 2. Atomic oxygen density (cm^{-3}) profiles for solar maximum (top panel) and solar minimum (bottom panel), for summer (x curves) and winter (solid curves), and for high (H) and low (L) geomagnetic activity. These profiles were calculated from the MSIS model of the neutral atmosphere [*Hedin et al.*, 1977*a*, *b*].

temperature, $\mathbf{U}_i$ is the drift velocity, $\mathbf{q}_i$ is the heat flow vector, $p_i = N_i k T_i$ is the partial pressure, and D_i/Dt is the total time derivative; similar definitions hold for species j. The other symbols are defined as follows: k is Boltzmann's constant, t is time, ∇ is the coordinate space gradient, ν_{ij} is the momentum transfer collision frequency between species i and j, and Φ_{ij} and Ψ_{ij} are velocity dependent correction factors. In (1), the summation is over the electrons and the neutrals N_2, O_2, O, He, and H. The relevant expressions for ν_{ij}, Φ_{ij}, and Ψ_{ij} are given by *Schunk and Nagy* [1980] and are not repeated here.

Several assumptions are implicit in (1), which was solved for O^+ ions. We have neglected the small temperature difference between the molecular and atomic ions in calculating the temperature coupling terms [cf. *Schunk et al.*, 1975]. We have also neglected viscous

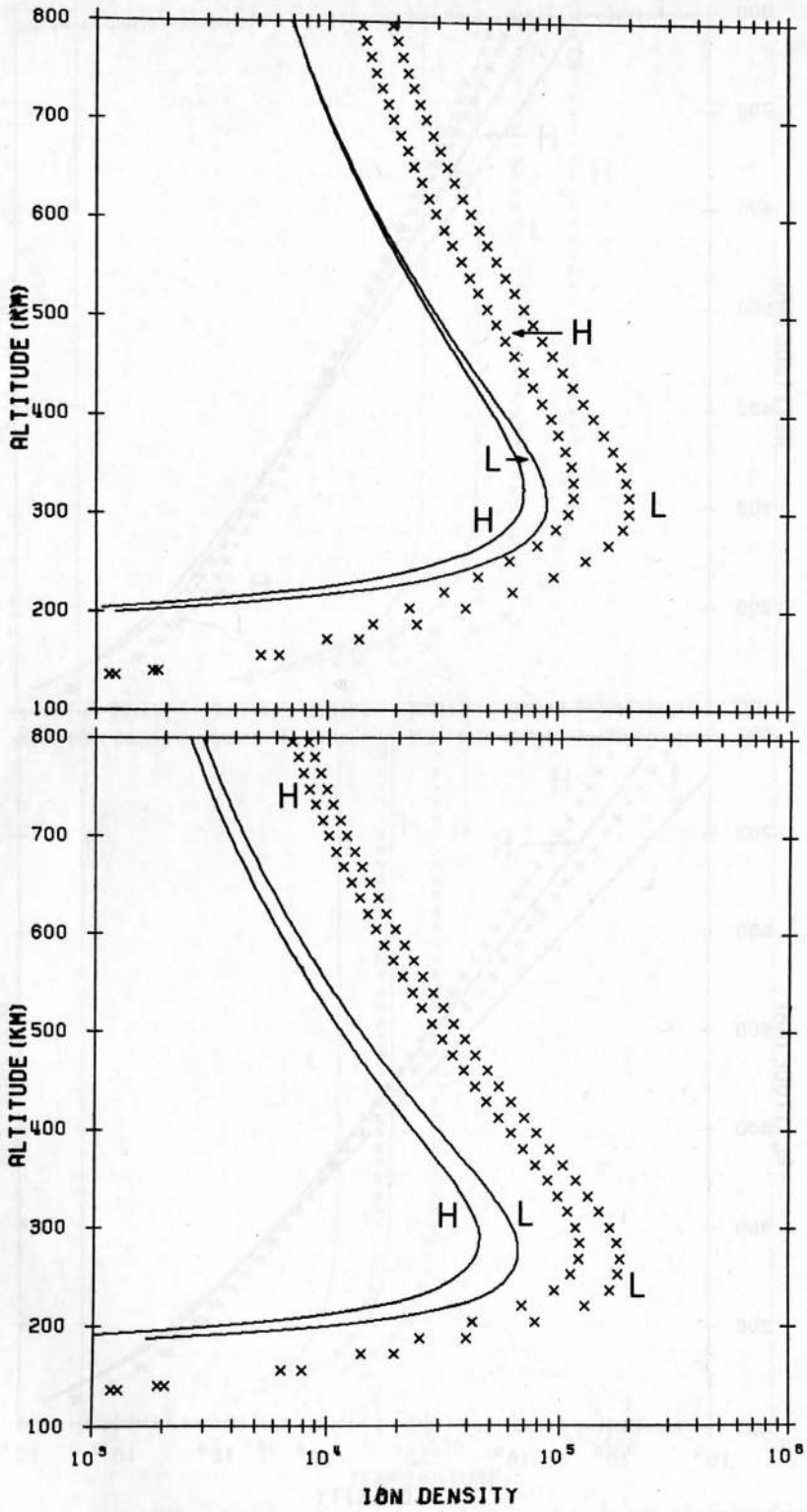

Fig. 3. O^+ density (cm^{-3}) profiles for solar maximum (top panel) and solar minimum (bottom panel), for summer (x curves) and winter (solid curves), and for high (H) and low (L) geomagnetic activity.

heating of the ion gas, which is typically much smaller than ion-neutral frictional heating. In addition, we have used the fact that the E x B ion motion is essentially incompressible [*Rishbeth and Hanson*, 1974]. These limitations should have a small effect on the results.

Recently, *Conrad and Schunk* [1979] have derived an expression for the ion heat flow vector which includes both thermal conduction and diffusion-thermal heat flow. This expression, which was derived for a collision-dominated, partially ionized, three-component plasma in thermal nonequilibrium, can be used at *F* region altitudes where the dominant species are electrons (subscript *e*),

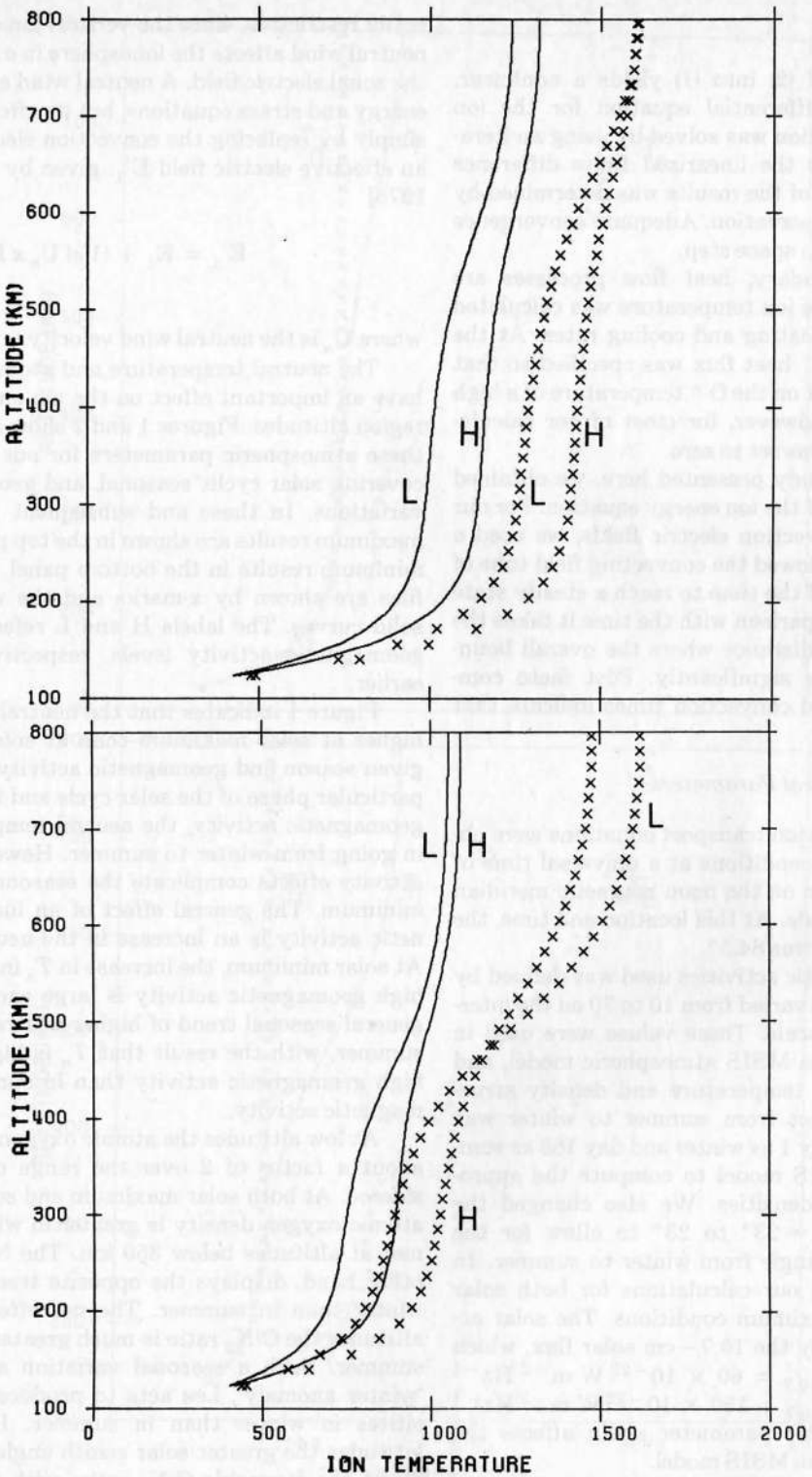

Fig. 4. O^+ temperature (°K) profiles for solar maximum (top panel) and solar minimum (bottom panel), for summer (x curves) and winter (solid curves), and for high (H) and low (L) geomagnetic activity.

ionized atomic oxygen (subscript i), and neutral atomic oxygen (subscript n). In the magnetic field direction, this expression takes the form

$$q_i = -K'_{ni}\nabla T_i - K_{in}\nabla T_n + R_{in}(U_i - U_n) \quad (2)$$

where K'_{ni} and K_{in} are thermal conductivities and R_{in} is the diffusion-thermal coefficient; these expressions are given by *Conrad and Schunk* [1979].

The O^+ heat flow expression (2) does not take account of O^+ collisions with the molecular ions (NO^+, O_2^+) and neutrals (N_2,O_2). However, such collisions are important only below about 250 km where heat flow effects are small.

2.2. Numerical Solution

The substitution of (2) into (1) yields a nonlinear, second-order, partial differential equation for the ion temperature. This equation was solved by using an iterative method applied to the linearized finite difference equation. The accuracy of the results was determined by checking the energy conservation. Adequate convergence was obtained with a 4 km space step.

At the lower boundary, heat flow processes are negligibly small, and the ion temperature was calculated by equating the local heating and cooling rates. At the upper boundary, the O^+ heat flux was specified so that we could study the effect on the O^+ temperature of a high altitude heat source. However, for most of our calculations the O^+ heat flux was set to zero.

For the daytime study presented here, we obtained steady state solutions of the ion energy equation. For our cases dealing with convection electric fields, we used a reference frame that followed the convecting field tube of plasma, which is valid if the time to reach a steady state solution is small in comparison with the time it takes the plasma to drift over a distance where the overall boundary conditions change significantly. Post facto comparisons of collision and convection times indicate that our solutions are valid.

2.3. Range of Geophysical Parameters

The solutions to the ion transport equations were obtained for steady state conditions at a universal time of 21.5 hours for a location on the noon magnetic meridian at 79°N magnetic latitude. At this location and time, the magnetic field dip angle was 84.5°.

The range of magnetic activities used was defined by the index A_p, which was varied from 10 to 70 on the internationally established scale. These values were used in the determination of the MSIS atmospheric model, and they affect the neutral temperature and density structure. The seasonal effect from summer to winter was specified by choosing day 1 as winter and day 183 as summer to enable the MSIS model to compute the appropriate neutral species densities. We also changed the solar declination from $-23°$ to $23°$ to allow for the change in solar zenith angle from winter to summer. In addition, we performed our calculations for both solar minimum and solar maximum conditions. The solar activities were specified by the 10.7 – cm solar flux, which was set to vary from $F_{10.7} = 60 \times 10^{-22}$ W m^{-2} Hz^{-1} for solar minimum to $F_{10.7} = 150 \times 10^{-22}$ W m^{-2} Hz^{-1} for solar maximum. This parameter again affects the neutral atmosphere in the MSIS model.

For each of the eight different geophysical conditions described above, we also considered the effect of a meridional electric field of 100 mV m^{-1} and zonal electric fields of ± 15 mV m^{-1}. A meridional electric field acts to increase the ion temperature, which affects the ion chemistry and plasma scale height. A zonal electric field, on the other hand, acts primarily to induce an upward or downward vertical ion drift, depending on the direction of the electric field. A vertical ion drift affects the electron density, which in turn alters the thermal coupling between the ions and electrons.

In all of our model calculations, we assumed that the neutral atmosphere was stationary. However, this is not really restrictive, since the vertical ion drift induced by a neutral wind affects the ionosphere in a manner similar to the zonal electric field. A neutral wind also affects the ion energy and stress equations, but its effect can be included simply by replacing the convection electric field $\mathbf{E}_\perp$ with an effective electric field $\mathbf{E}'_\perp$, given by [cf. *Schunk et al.*, 1975]

$$\mathbf{E}'_\perp = \mathbf{E}_\perp + (1/c)\,\mathbf{U}_n \times \mathbf{B} \tag{3}$$

where $\mathbf{U}_n$ is the neutral wind velocity.

The neutral temperature and atomic oxygen density have an important effect on the ion energy balance at F region altitudes. Figures 1 and 2 show altitude profiles of these atmospheric parameters for our eight basic cases covering solar cycle, seasonal, and geomagnetic activity variations. In these and subsequent figures, the solar maximum results are shown in the top panel and the solar minimum results in the bottom panel. The summer profiles are shown by x-marks and the winter profiles by solid curves. The labels H and L refer to high and low geomagnetic activity levels, respectively, as specified earlier.

Figure 1 indicates that the neutral temperatures are higher at solar maximum than at solar minimum for a given season and geomagnetic activity level. Also, for a particular phase of the solar cycle and for a given level of geomagnetic activity, the neutral temperature increases in going from winter to summer. However, geomagnetic activity effects complicate the seasonal picture at solar minimum. The general effect of an increase in geomagnetic activity is an increase in the neutral temperature. At solar minimum, the increase in T_n in going from low to high geomagnetic activity is large enough to offset the general seasonal trend of higher neutral temperatures in summer, with the result that T_n is higher in winter for high geomagnetic activity than in summer for low geomagnetic activity.

At low altitudes the atomic oxygen density varies by about a factor of 2 over the range of conditions considered. At both solar maximum and solar minimum, the atomic oxygen density is greater in winter than in summer at altitudes below 350 km. The N_2 density, on the other hand, displays the opposite trend, being lower in winter than in summer. The net effect is that at low altitudes the O/N_2 ratio is much greater in winter than in summer. Such a seasonal variation acts to produce a 'winter anomaly', i.e., acts to produce greater O^+ densitites in winter than in summer. However, at high latitudes the greater solar zenith angle in winter acts to offset the favorable O/N_2 ratio, with the result that at winter solstice the 'winter anomaly' does not occur [cf. *Schunk and Raitt*, 1980].

3. ION TEMPERATURE VARIATIONS

We studied how the daytime ion temperature in the high-latitude F region varies with season, solar cycle, geomagnetic activity, convection electric field strength, the vertical ionization drift velocity, and an assumed downward heat flux at high altitudes. The various cases will be discussed separately in the subsections that follow.

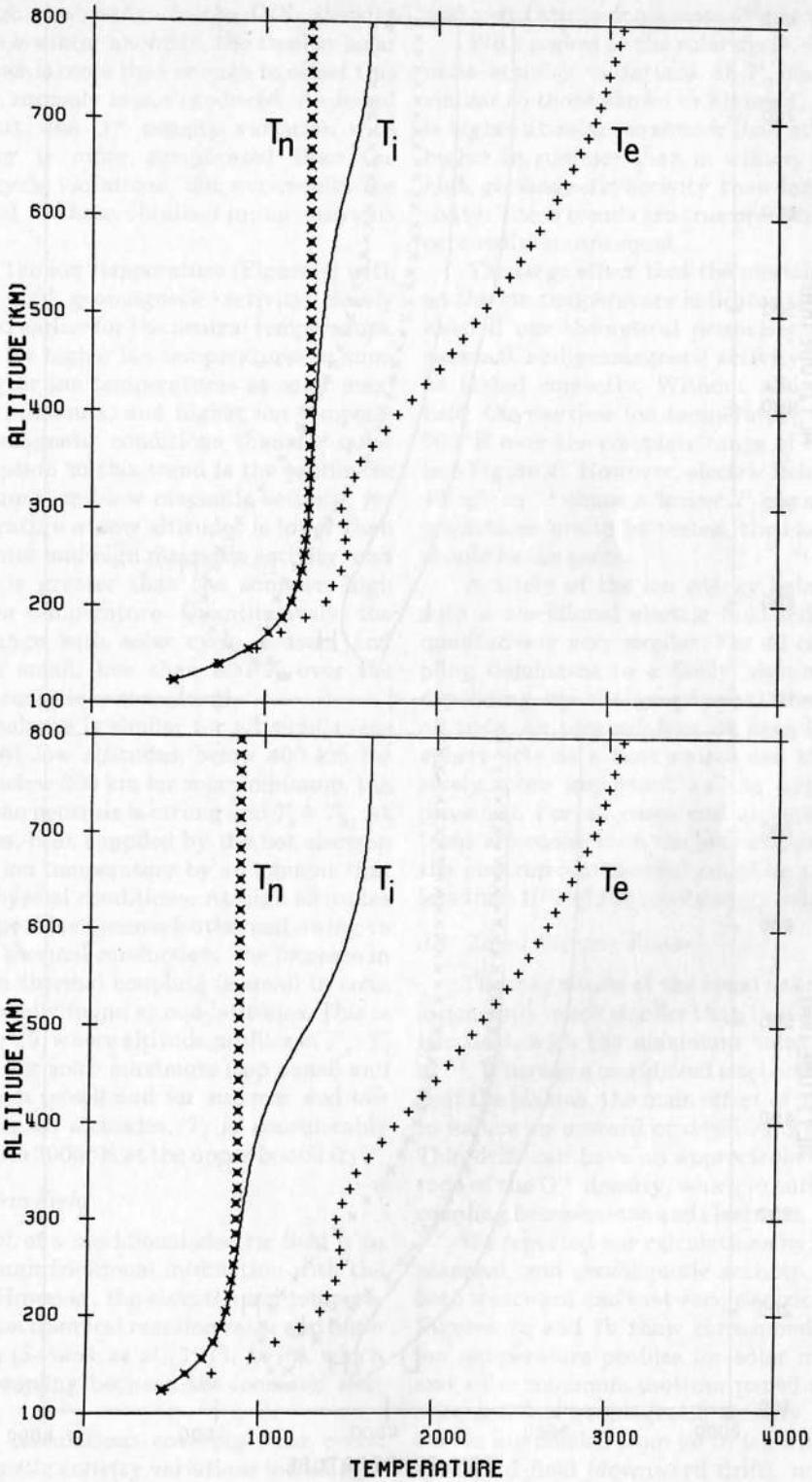

Fig. 5. O^+, electron and neutral temperature (°K) profiles for solar maximum (top panel) and solar minimum (bottom panel) and for summer and low geomagnetic activity.

3.1. Solar Cycle, Seasonal, and Geomagnetic Activity Variations

The electron density and ion temperature profiles for the different solar cycle, seasonal, and geomagnetic activity conditions that we considered are shown in Figures 3 and 4, respectively. It should be noted that the geographic location we selected for this study is not the same as that used in our previous daytime study [*Schunk and Raitt*, 1980]. In the Schunk and Raitt study the ionosphere was in darkness below 300 km in winter, whereas in this study the F region remains sunlit at all altitudes for all geophysical conditions. Nevertheless, the solar cycle, seasonal, and geomagnetic activity variations of the

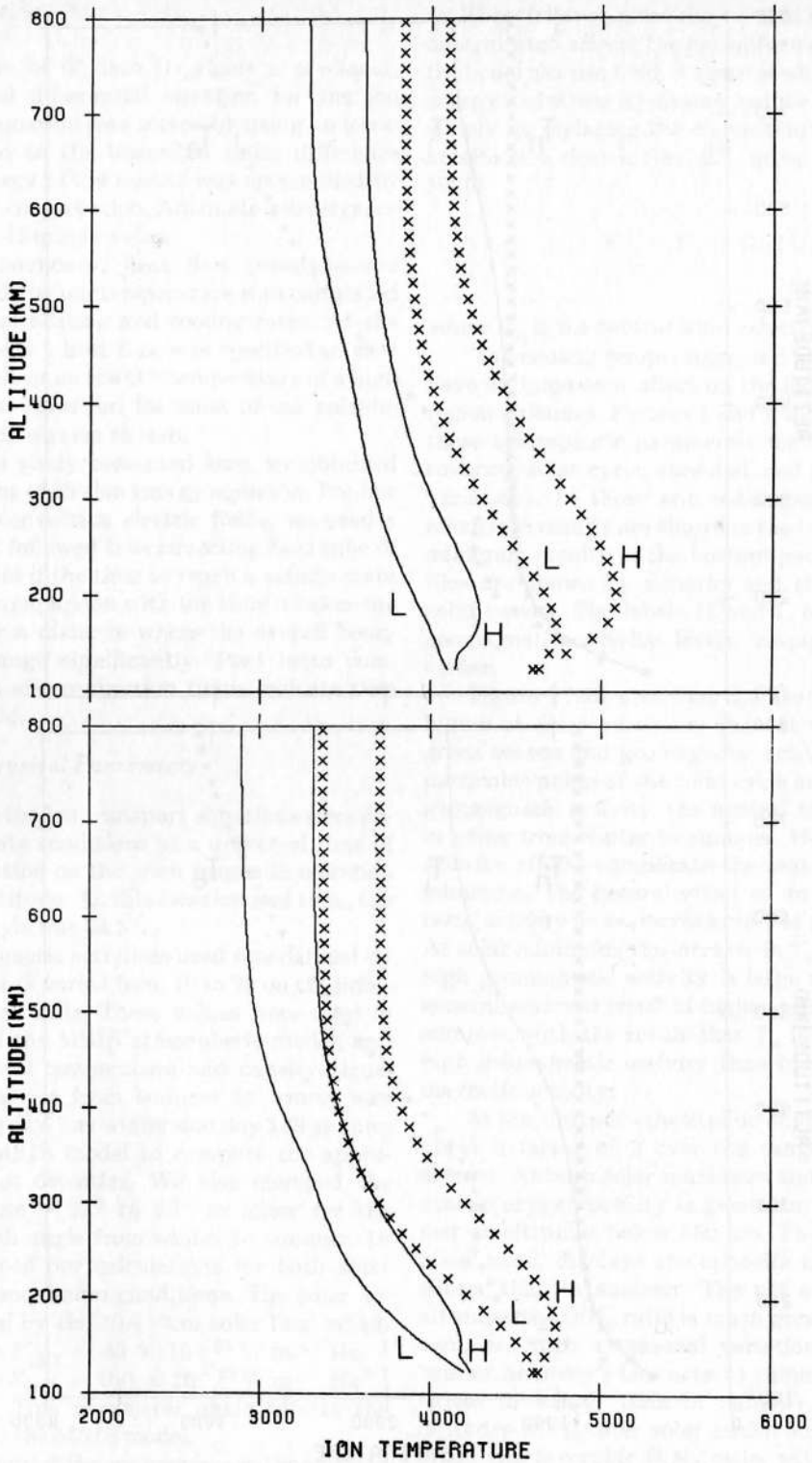

Fig. 6. O^+ temperature (°K) profiles for a meridional electric field of 100 mV m^{-1}. The profiles were calculated for solar maximum (top panel) and solar minimum (bottom panel), for summer (x curves) and winter (solid curves), and for high (H) and low (L) geomagnetic activity.

O^+ density shown in Figure 3 are qualitatively the same as those obtained by *Schunk and Raitt* [1980].

Briefly, the solar cycle trend is for higher N_mF_2 and h_mF_2 values at solar maximum than at solar minimum. Also, above the F region peak the O^+ density is greater at solar maximum. The seasonal variation yields higher O^+ densities in summer than in winter, with the exact difference depending on the other geophysical conditions. Typically, the seasonal O^+ density variation was greater at the location selected by *Schunk and Raitt* [1980] because the ionosphere was in darkness below 300 km in winter, which resulted in lower winter O^+ densities in

that study. Although the change in the O/N_2 density ratio acts to produce a winter anomaly, the smaller solar zenith angle in summer is more than enough to offset this change and a winter anomaly is not produced. As found by Schunk and Raitt, the O^+ density variation with geomagnetic activity is more complicated than the seasonal and solar cycle variations, but our results are qualitatively identical to those obtained in our previous study.

The variation of the ion temperature (Figure 4) with solar cycle, season, and geomagnetic activity closely follows that discussed earlier for the neutral temperature. The general trend is for higher ion temperatures in summer than winter, higher ion temperatures at solar maximum than at solar minimum, and higher ion temperatures for active geomagnetic conditions than for quiet conditions. The exception to this trend is the profile for solar minimum, summer, and low magnetic activity, for which the ion temperature at low altitudes is lower than that obtained for winter and high magnetic activity, and at high altitudes it is greater than the summer, high magnetic activity ion temperature. Quantitatively, the ion temperature change with solar cycle, season, and magnetic activity is small, less than 600°K over the range of geophysical conditions considered.

The ion energy balance is similar for all eight cases shown in Figure 4. At low altitudes, below 400 km for solar maximum and below 300 km for solar minimum, the thermal coupling to the neutrals is strong and $T_i \cong T_n$. At intermediate altitudes, heat supplied by the hot electron gas acts to raise the ion temperature by an amount that depends on the geophysical conditions. At high altitudes the ion temperature profiles become isothermal owing to the dominance of ion thermal conduction. The increase in T_i due to ion-electron thermal coupling is small in comparison with that normally found at mid-latitudes. This is clearly shown in Figure 5, where altitude profiles of T_n, T_i and T_e are presented for solar maximum (top panel) and solar minimum (bottom panel) and for summer and low magnetic activity. At all altitudes, T_i is considerably below T_e, which reaches 3000°K at the upper boundary.

3.2. *Meridional Electric Field*

The primary effect of a meridional electric field is to heat the plasma through fricitional interaction with the neutral atmosphere. However, the elevated ion temperatures act to alter the ion chemical reaction rates and high-altitude scale heights [*Schunk et al.*, 1975, 1976], which affects the thermal coupling between the ions and electrons.

We repeated our calculations covering solar cycle, seasonal, and geomagnetic activity variations including a 100 mV m^{-1} meridional electric field and the resulting ion temperature profiles are shown in Figure 6. With allowance for the 100 mV m^{-1} electric field, the ion temperatures are significantly enhanced at all altitudes and the altitude profiles are considerably different from those obtained without the electric field (compare Figures 4 and 6). For all eight cases, the altitude variation of T_i is similar. High ion temperatures occur at low altitudes owing to the frictional interaction between ions and neutrals. Above the temperature maxima, T_i decreases with altitude, which follows the decrease in the frictional heating rate. At high altitudes the T_i profiles are isothermal owing to the dominance of thermal conduction.

With regard to the solar cycle, seasonal, and geomagnetic activity variations of T_i, the general trends are similar to those shown in Figure 4. At most altitudes, T_i is higher at solar maximum than at solar minimum, T_i is higher in summer than in winter, and T_i is greater for high geomagnetic activity than for low geomagnetic activity. These trends are true provided the other geophysical conditions are equal.

The large effect that the meridional electric field has on the ion temperature indicates that care must be exercised if our theoretical predictions for the solar cycle, seasonal, and geomagnetic activity variations of T_i are to be tested correctly. Without allowance for an electric field, the daytime ion temperature changes by less than 600°K over the complete range of conditions considered (see Figure 4). However, electric fields greater than about 40 mV m^{-1} cause a larger T_i change. Therefore, if our predictions are to be tested, the electric field conditions should be the same.

A study of the ion energy balances for these cases with a meridional electric field indicates that they are qualitatively very similar. For all cases, ion-neutral coupling dominates to a fairly high altitude, 500-700 km depending on the geophysical conditions. Above this altitude, an upward flow of heat from the lower ionosphere acts as a heat source and this becomes progressively more important as the upper boundary is approached. For all cases and at most altitudes, the electrons are cooler than the ions and act as a heat sink, but the electron-ion thermal coupling typically amounts to less than 10% of the total energy balance.

3.3. *Zonal Electric Fields*

The magnitude of the zonal or east-west electric field is generally much smaller than that of the meridional electric field, with the maximum value being about 30 mV m^{-1}. Whereas a meridional electric field acts primarily to heat the plasma, the main effect of a zonal electric field is to induce an upward or downward electrodynamic drift. This drift can have an appreciable effect on the magnitude of the O^+ density, which in turn affects the thermal coupling between ions and electrons.

We repeated our calculations by covering solar cycle, seasonal, and geomagnetic activity variations including both westward and eastward electric fields of 15 mV m^-. Figures 7a and 7b show corresponding O^+ density and ion temperature profiles for solar maximum (top panel) and solar minimum (bottom panel) and for summer solstice and low geomagnetic activity. In both figures the curves are labeled from (*a*) to (*c*), which corresponds to a westward field (downward drift), no field, and an eastward field (upward drift), respectively. The progression from a downward drift to no drift, to an upward drift leads to an increase in both N_mF_2 and h_mF_2. This simply results from the fact that an upward drift raises the F layer to an altitude where the loss rate is lower, and hence, the O^+ density is increased.

The increase in the O^+ density in going from a downward drift to no drift, to an upward drift also leads to an increased thermal coupling between ions and electrons, which results in elevated ion temperatures at high altitudes. For the downward drift $N_mF_2 \sim 10^5$ cm^{-3} and the thermal coupling to the electrons is very small, with

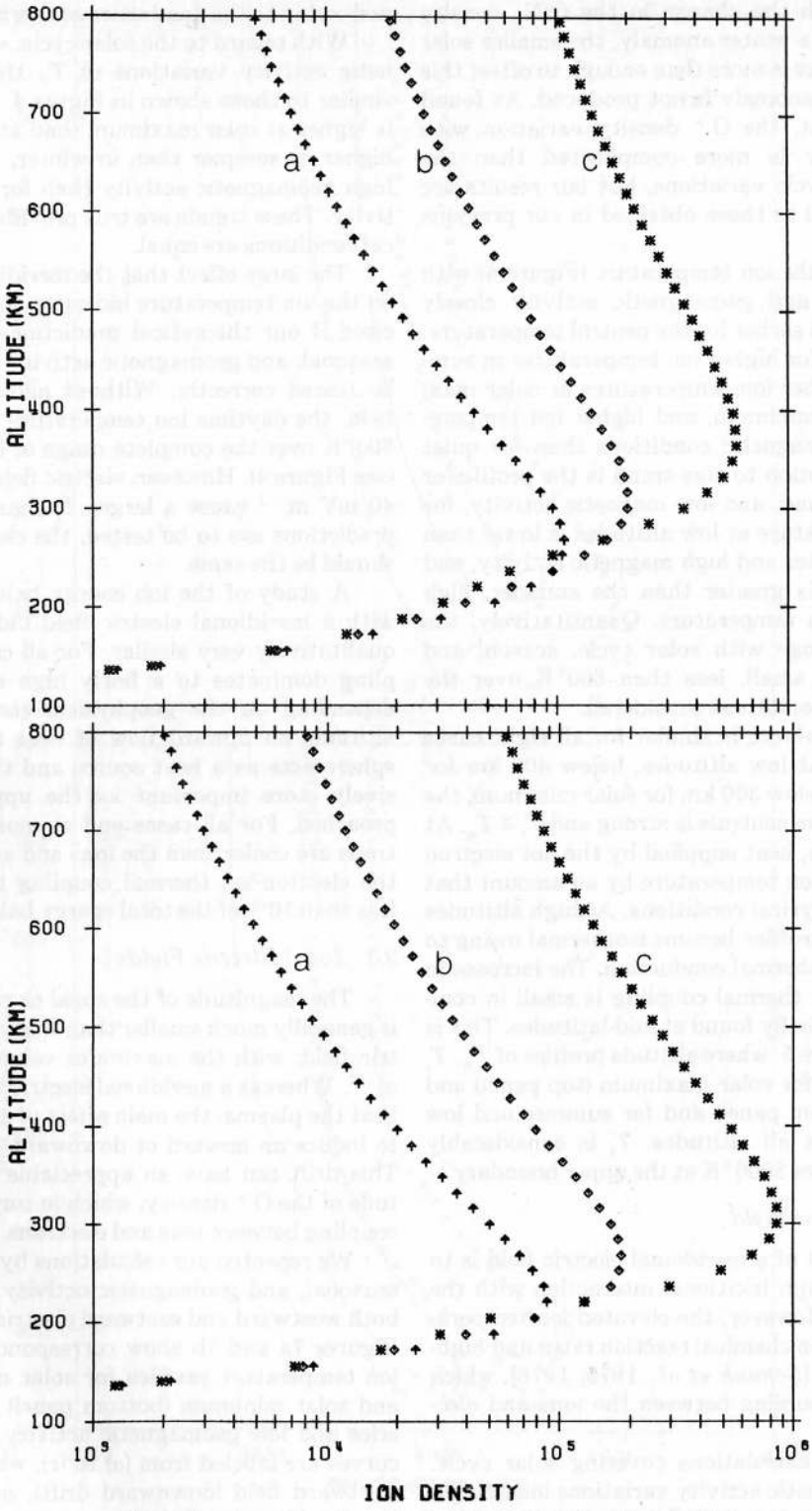

Fig. 7*a*. O^+ density (cm^{-3}) profiles for several zonal electric fields. The electric fields are (*a*) 15 mV m^{-1} westward, (*b*) O mV m^{-1}, and (*c*) 15 mV m^{-1} eastward. The profiles were calculated for solar maximum (top panel) and solar minimum (bottom panel) and for summer and low geomagnetic activity.

the result that $T_i \cong T_n$ at all altitudes for both solar maximum and solar minimum. For the upward drift, on the other hand, $N_m F_2 \sim 10^6$ cm^{-3} and the ion-electron thermal coupling is fairly strong. At solar minimum, $T_i \cong$ 2700 °K at high altitudes, while $T_e \cong 3000$ °K.

As was found for a meridional electric field, the change in the ion temperature due to a change in the zonal electric field can be larger than that associated with the solar cycle, seasonal and geomagnetic activity variations, which is less than 600 °K.

3.4. *Effect of Topside O^+ Heat Flux*

Energetic O^+ ions are commonly observed at high altitudes over the polar regions. However, it is not clear

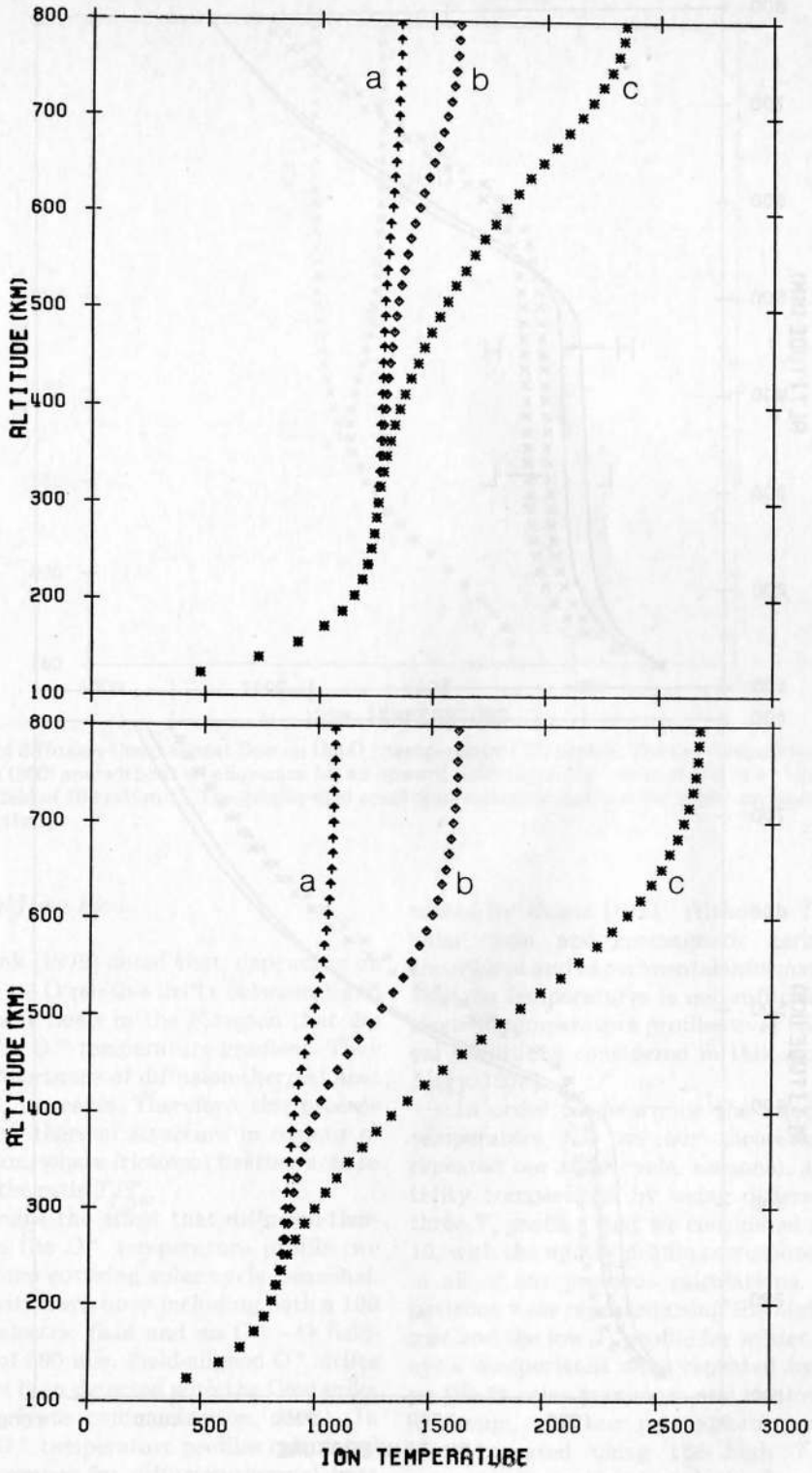

Fig. 7*b*. O^+ temperature (°K) profiles for several zonal electric fields. These temperature profiles correspond to the O^+ density profiles shown in Figure 7*a*.

whether or not these ions act as a high altitude heat source for the thermal O^+ ions at lower altitudes. To determine their possible effect on the F region ion temperature, we repeated our solar cycle, seasonal, and geomagnetic activity calculations assuming a downward O^+ heat flux of 4×10^{-4} erg cm^{-2} s^{-1} at our upper boundary. Figure 8 shows the resulting ion temperature profiles. An important feature to note is that a topside heat source can affect the T_i profile to a much lower altitude at high latitudes than a middle and low latitudes, where a topside heat source typically does not affect T_i below 600-700 km [*Banks and Kockarts*, 1973; *Rees and Roble*, 1975]. At high latitudes, a topside ion heat source can penetrate to lower altitudes because of the lower elec-

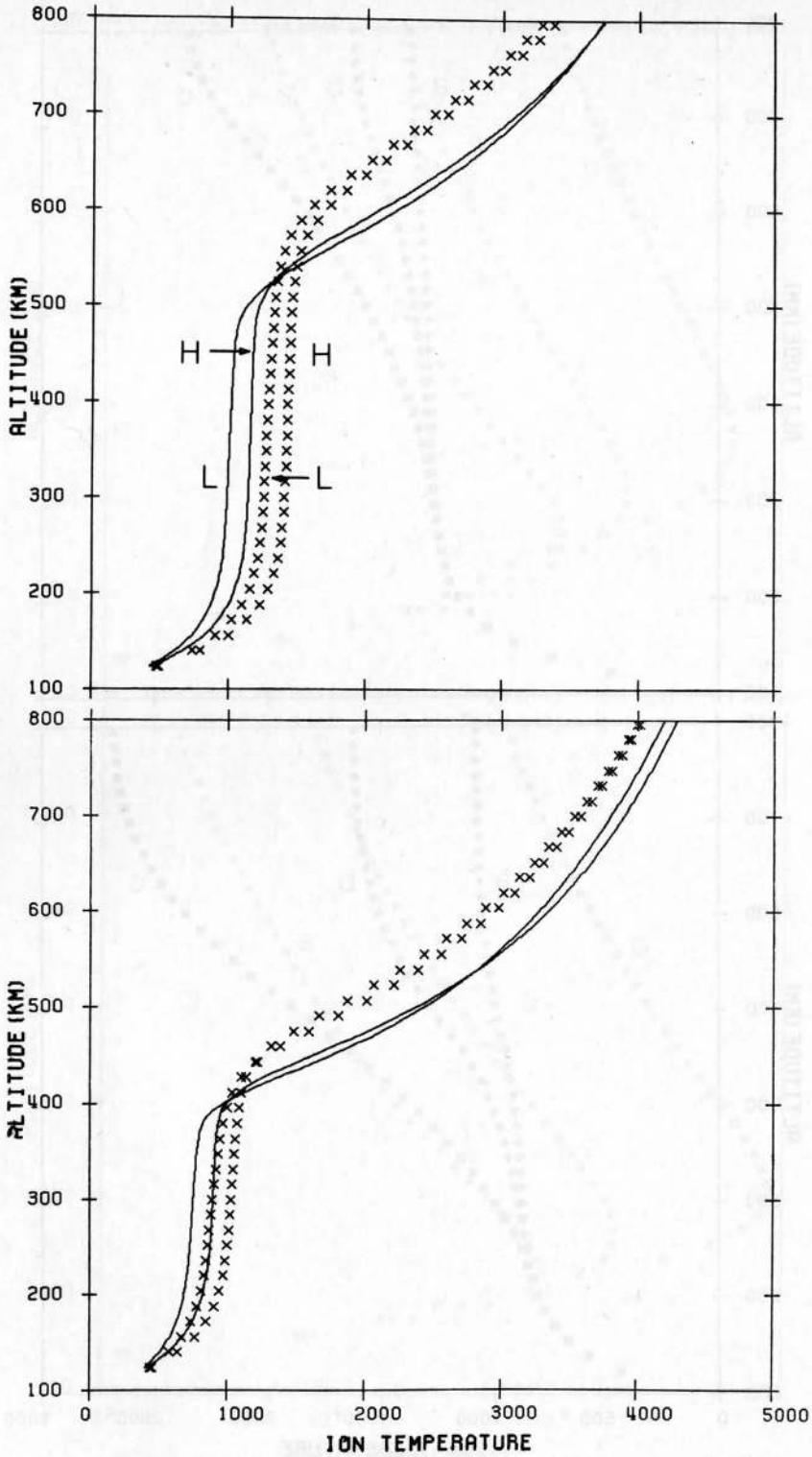

Fig. 8. O^+ temperature (°K) profiles for a topside heat flux of -4×10^{-4} erg $cm^{-2}s^{-1}$. These profiles were calculated for solar maximum (top panel) and solar minimum (bottom panel), for summer (x curves) and winter (solid curves), and for high (H) and low (L) geomagnetic activity. At solar minimum there is a very small difference between the O^+ temperature profiles for high and low geomagnetic activity.

tron densities, which act to increase the importance of thermal conduction relative to ion-electron thermal coupling.

With regard to the penetration of the O^+ heat flow to low altitudes as a function of solar activity, it can affect T_i to a lower altitude at solar minimum than at solar maximum. It also penetrates to a lower altitude in winter than in summer. However, there is little difference in the altitude of penetration for high and low geomagnetic activity. This general behavior is simply related to the electron density variation, with lower electron densities allowing the O^+ heat flow to penetrate to lower altitudes.

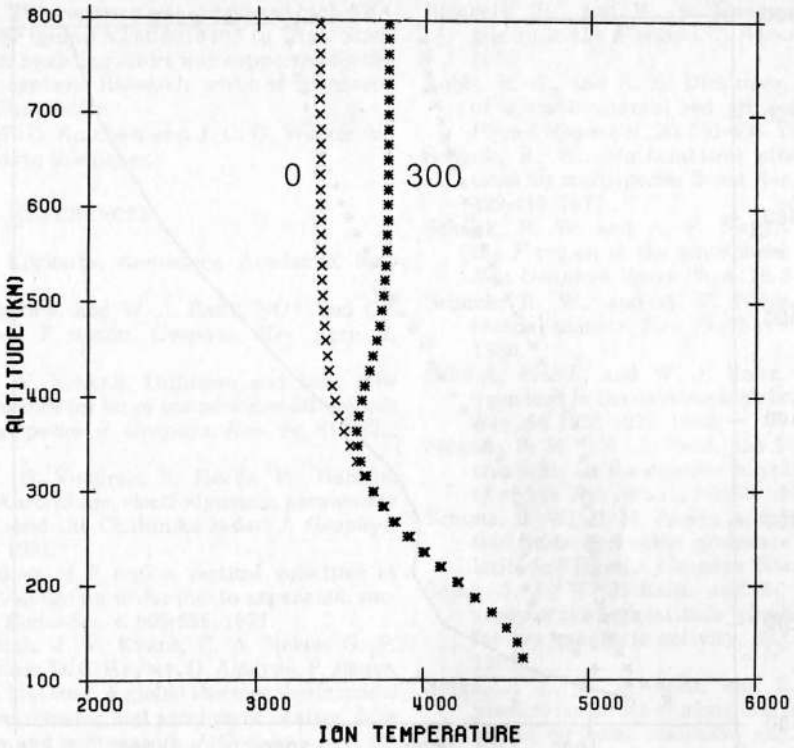

Fig. 9. Effect of diffusion-thermal heat flow on the O^+ temperature (°K) profile. The O^+ temperature profile was calculated with (300) and without (0) allowance for an upward field-aligned O^+ drift of 300 m s^{-1} and for a meridional electric field of 100 mV m^{-1}. The geophysical conditions corresponded to solar minimum, summer, and low geomagnetic activity.

3.5. *Diffusion-Thermal Heat Flow*

Conrad and Schunk [1979] noted that, depending on altitude and T_i/T_n, $O^+ - O$ relative drifts between 1 and 300 m/s induce O^+ heat flows in the F region that are equivalent to a 1 °K/km O^+ temperature gradient. They also noted that the importance of diffusion-thermal heat flow increases as T_i/T_n increases. Therefore, this process could influence the O^+ thermal structure in regions of rapid plasma convection, where frictional heating acts to increase significantly the ratio T_i/T_n.

In order to determine the effect that diffusion-thermal heat flow has on the O^+ temperature profile, we repeated our calculations covering solar cycle, seasonal, and geomagnetic activity variations including both a 100 mV m^{-1} meridional electric field and an $O^+ - O$ field-aligned relative drift of 300 m/s. Field-aligned O^+ drifts of this magnitude have been detected with the Chatanika radar (J.C. Foster, private communication, 1981). In Figure 9 we compare O^+ temperature profiles calculated with and without allowance for diffusion-thermal heat flow for a typical case. It is apparent that diffusion-thermal heat flow has a small effect on the O^+ thermal structure, with the O^+ temperature at high altitudes being increased by about 500 °K due to the upward O^+ drift of 300 m/s.

3.6. *Electron Temperature Distribution*

As in our previous studies, we did not attempt to solve the electron energy balance equation in order to obtain electron temperatures. Instead, a representative electron temperature profile was adopted from measurements by *Evans* [1971]. Although T_e exhibits seasonal, solar cycle, and geomagnetic variations, the current theoretical and experimental information on high-latitude electron temperatures is not sufficient to obtain reliable electron temperature profiles over the range of geophysical conditions considered in this study [cf. *Schunk and Nagy*, 1978].

In order to determine the effect that the electron temperature has on our theoretical predictions, we repeated our solar cycle, seasonal, and geomagnetic activity comparisons by using different T_e profiles. The three T_e profiles that we considered are shown in Figure 10, with the middle profile corresponding to the one used in all of our previous calculations. Our seasonal comparisons were repeated using the high T_e profile for summer and the low T_e profile for winter. Likewise, our solar cycle comparisons were repeated by using the high T_e profile at solar maximum and the low T_e profile at solar minimum, and our geomagnetic activity comparisons were repeated using the high T_e profile for high geomagnetic activity and the low T_e profile for low geomagnetic activity. Not only were the seasonal, solar cycle, and geomagnetic activity variations of T_i qualitatively the same, but the trends were enhanced. However, the enhancement was slight, with the largest change in T_i for all of the cases being less than 200 °K.

The main conclusion to be drawn from the above study is that, in general, the electron temperature does not have a significant effect on the ion temperature in the daytime high-latitude F region. This result is in sharp contrast to that obtained at middle and low latitudes where T_e has a strong influence on T_i [cf. *Banks and*

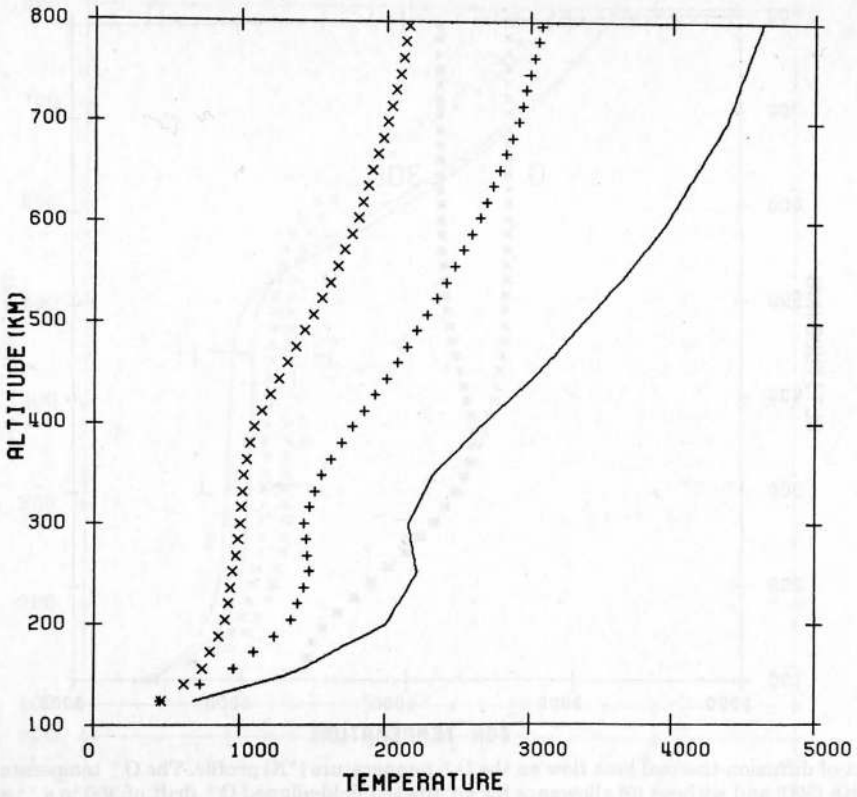

Fig. 10. Electron temperature (°K) profiles used in the calculations. The middle profile corresponds to our standard electron temperature profile.

Kockarts, 1973]. This difference results because at high latitudes the ion-electron thermal coupling is small owing to the low electron densities.

Although we did not calculate nighttime T_i profiles, the ion-electron thermal coupling should be even smaller on the nightside than on the dayside because of the lower electron densities. Therefore, in the high-latitude ionosphere outside of the auroral oval, the electron temperature should have a small effect on the ion temperature for a wide range of geophysical conditions.

4. SUMMARY

We improved our high-latitude ionospheric model by including thermal conduction and diffusion-thermal heat flow terms in the ion energy equation so that we could study the ion temperature variations in the daytime high-latitude F region. We studied the ion temperature variation with season, solar cycle, geomagnetic activity, convection electric field, a vertical ionization drift velocity, and a downward heat flux at high altitudes.

From our study we found the following:

1. The variation of T_i with solar cycle, season, and geomagnetic activity closely follows the T_n variation. The general trend is for higher ion temperatures in summer than in winter, higher ion temperatures at solar maximum than at solar minimum, and higher ion temperatures for active geomagnetic conditions than for quiet conditions. However, there are exceptions to this general trend. Quantitatively, the T_i change with solar cycle, season, and geomagnetic activity is small, less than 600 °K over the range of conditions considered.

2. At low altitudes the ion energy balance is determined by thermal coupling to the neutrals. At intermediate altitudes coupling to the electrons becomes appreciable, and at high altitudes ion thermal conduction dominates.

3. A meridional electric field produces elevated ion temperatures through frictional interaction between ions and neutrals. Although the heating occurs predominately at low altitudes, there is an upward flow of heat from the lower ionosphere which acts to raise the ion temperature at high altitudes. Typically, meridional electric fields greater than 40 mV m^{-1} can cause a T_i change that is larger than that due to solar cycle, seasonal, and geomagnetic activity changes.

4. Zonal electric fields affect T_i indirectly through changes in the electron density, which affects the ion-electron thermal coupling. A westward electric field induces a downward ionization drift, which results in a low electron density and a smaller thermal coupling. The reverse occurs for an eastward field. The change in T_i due to a change in the zonal electric field can be larger than that associated with the solar cycle, seasonal, and geomagnetic activity variations.

5. The effects of a topside ion heat source can penetrate to a much lower altitude at high latitudes than at middle and low latitudes.

6. Diffusion-thermal heat flow has its greatest effect on T_i in regions of rapid plasma convection, where T_i can be increased by at most 500 °K due to this process.

7. In general, T_e has a much smaller effect on T_i at high latitudes than at mid-latitudes owing to the smaller electron densities and hence reduced ion-electron thermal coupling.

Acknowledgements. This research was supported by NASA grant NAGW-77 and NSF grant ATM-8015497 to Utah State University. The computer modeling effort was supported by the National Center for Atmospheric Research, which is sponsored by the National Science Foundation.

The Editor thanks W. C. Knudsen and J. C. G. Walker for their assistance in evaluating this paper.

REFERENCES

Banks, P. M., and G. Kockarts, *Aeronomy*, Academic, New York, 1973.

Banks, P. M., R. W. Schunk, and W. J. Raitt, NO^+ and O^+ in the high latitude *F* region, *Geophys. Res. Lett., 1*, 239-242, 1974.

Conrad, J. R., and R. W. Schunk, Diffusion and heat flow equations with allowance for large temperature differences between interacting species, *J. Geophys. Res., 84*, 811-822, 1979.

De la Beaujardiere, O., R. Vondrak, R. Heelis, W. Hanson, and R. Hoffman, Auroral arc electrodynamic parameters measured by AE-C and the Chatanika radar, *J. Geophys. Res., 86*, 4671-4685, 1981.

Evans, J. V., Observations of *F* region vertical velocities at Millstone Hill, 1, Evidence for drifts due to expansion, contraction and winds, *Radio Sci., 6*, 609-626, 1971.

Hedin, A. E., J. E. Salah, J. V. Evans, C. A. Reber, G. P. Newton, N. W. Spencer, D. C. Kayser, D. Alcayde, P. Bauer, L. Cogger, and J. P. McClure, A global thermospheric model based on mass spectrometer and incoherent scatter data MSIS, 1, N_2 density and temperature, *J. Geophys. Res., 82*, 2139-2147, 1977*a*.

Hedin, A. E., C. A. Reber, G. P. Newton, N. W. Spencer, H. C. Brinton, H. G. Mayr, and W. E. Potter, A global thermospheric model based on mass spectrometer and incoherent scatter data MSIS, 2, Composition, *J. Geophys. Res., 82*, 2148-2156, 1977*b*.

Kelley, J. D. and V. B. Wickwar, Radar measurements of high-latitude ion composition between 140 and 300 km altitude, *J. Geophys. Res., 86*, 7617-7626, 1981.

Knudsen, W. C., P. M. Banks, J. D. Winningham, and D. M. Klumpar, Numerical model of the convection F_2 ionosphere at high latitudes, *J. Geophys. Res., 82*, 4784, 1977.

Rees, M. H., and R. G. Roble, Observations and theory of the formation of stable auroral red arcs, *Rev. Geophys. Space Phys., 13*, 201-242, 1975.

Rees, M. H., and J. C. G. Walker, Ion and electron heating by auroral electric fields, *Ann. Geophys, 24*, 193-199, 1968.

Rees, M. H., R. G. Roble, J. Kopp, A. J. Abreu, L. H. Brace, H. C. Brinton, R. A. Heelis, R. A. Hoffman, D. C. Kayser, and D. W. Rusch, The spatial-temporal ambiguity in auroral modeling, *J. Geophys. Res., 85*, 1235-1245, 1980.

Rishbeth, H., and W. B. Hanson, A comment on plasma pile-up in the *F* region, *J. Atmos. Terr. Phys., 36*, 703-706, 1974.

Roble, R. G., and R. E. Dickinson, Time dependent behavior of a stable auroral red arc excited by an electric field, *Planet. Space Sci., 20*, 591-605, 1972.

Schunk, R. W., Mathematical structure of transport equations for multispecies flows, *Rev. Geophys. Space Phys., 15*, 429-445, 1977.

Schunk, R. W. and A. F. Nagy, Electron temperatures in the *F* region of the ionosphere: Theory and observations, *Rev. Geophys. Space Phys., 16*, 355-399, 1978.

Schunk, R. W., and A. F. Nagy, Ionospheres of the terrestrial planets, *Rev. Geophys. Space Phys., 18*, 813-852, 1980.

Schunk, R. W., and W. J. Raitt, Atomic nitrogen and oxygen ions in the daytime high-latitude *F* region, *J. Geophys. Res., 85*, 1255-1272, 1980.

Schunk, R. W. , W. J. Raitt, and P. M. Banks, Effect of electric fields on the daytime high-latitude *E* and *F* regions, *J. Geophys. Res., 80*, 3121-3130, 1975.

Schunk, R. W., P. M. Banks, and W. J. Raitt, Effects of electric fields and other processes upon the nighttime high-latitude *F* layer, *J. Geophys. Res., 81*, 3271-3282, 1976.

Sojka, J. J., W. J. Raitt, and R. W. Schunk, A theoretical study of the high-latitude winter *F* region at solar minimum for low magnetic activity, *J. Geophys Res., 86*, 609-621, 1981*a*.

Sojka, J. J., W. J. Raitt, and R. W. Schunk, Theoretical predictions for ion composition in the high-latitude winter *F* region for solar minimum and low magnetic activity, *J. Geophys. Res., 86*, 2206-2216, 1981*b*.

St.-Maurice, J.-P., W. B. Hanson and J. C. G. Walker, Retarding potential analyzer measurement of the effect of ion-neutral collisions on the ion velocity distribution in the auroral ionosphere, *J. Geophys. Res., 81*, 5438-5446, 1976.

St.-Maurice, J.-P., and W. B. Hanson, A determination of *F* region neutral winds through their effects on ion frictional heating at high latitudes, submitted to *J. Geophys. Res.*, 1982.

Watkins, B. J., A numerical computer investigation of the polar *F* region ionosphere, *Planet. Space Sci., 26*, 559-569, 1978.

Wakins, B. J., and P. M. Banks, A preliminary study of high-latitude thermospheric temperatures from incoherent scatter radar observations, *J. Geophys. Res., 79*, 5307-5310, 1974.

(Received January 25, 1982;
revised March 26, 1982;
accepted March 29, 1982.)